

# ON THE USE OF MULTI-FREQUENCY SAR DATA TO IMPROVE THE MONITORING OF INTERTIDAL FLATS ON THE GERMAN NORTH SEA COAST

Martin Gade<sup>(1)</sup>, Kerstin Stelzer<sup>(2)</sup>, Jörn Kohlus<sup>(3)</sup>

<sup>(1)</sup>*Universität Hamburg, ZMAW, Institut für Meereskunde, Bundesstraße 53, 20146 Hamburg, Germany, Email: martin.gade@zmaw.de*

<sup>(2)</sup>*Brockmann Consult GmbH, Geoinformation Services, Max-Planck-Str. 2, 21502 Geesthacht, Germany, Email: kerstin.stelzer@brockmann-consult.de*

<sup>(3)</sup>*Landesbetrieb für Küstenschutz, Nationalpark und Meeresschutz Schleswig-Holstein - Nationalparkverwaltung, Schlossgarten 1, 25832 Tönning, German, Email: Joern.Kohlus@lkn.landsh.de*

## ABSTRACT

We demonstrate that Synthetic Aperture Radar (SAR) data have great potential to improve an existing monitoring system for intertidal flats and to complement the classification of sediments, macrophytes, and mussels in the German Wadden Sea. Multi-satellite SAR data acquired at different radar bands (L, C, and X band, from ALOS PALSAR, from ERS SAR, Radarsat-2 and ENVISAT ASAR, and from TerraSAR-X, respectively) were used to analyse their potential for crude sediment classification on dry-fallen intertidal flats and for detecting benthic fauna such as blue mussel or oyster beds. We show that both multi-satellite and multi-temporal analyses provide valuable input for the routine monitoring of exposed intertidal flats on the German North Sea Coast. In addition, we demonstrate that high-resolution SAR is capable of detecting residuals of historical land use in areas that were lost to the sea during major storm surges in the 13<sup>th</sup> and 17<sup>th</sup> centuries.

## 1. INTRODUCTION

The largest intertidal flats can be found on the German and Dutch North Sea coast and on the western coast of South Korea, in a distance of up to 10 Km offshore. Those areas fall dry once during each tidal cycle and consist of fine sediments such as (fine) sand and mud, and they are only partly vegetated. Not only because they are impacted by the stress of a changing world (e.g. through the global sea level rise and the expected increasing frequency of storm events) a frequent surveillance is of great importance, but is a difficult task by boat, foot, or land vehicles. This is when remote sensing techniques come into play.

High-resolution multispectral remote sensing data from satellite-borne optical sensors are already being used for the classification of sediments, macrophytes, and mussels on exposed intertidal flats in the German Wadden Sea. Since the use of those sensors in northern latitudes is strongly limited by clouds and haze, we included SAR data, allowing for an observation of intertidal flats that is independent of cloud coverage and daytime.

Gade et al. (2008) suggested using multi-frequency SAR data for a sediment classification on exposed intertidal flats. They demonstrated that pairs of simultaneously acquired L-, C- and X-band SAR images from the SIR-C/X-SAR campaigns in 1994 can be used for a crude sediment classification based on the inversion of the Integral Equation Model, IEM (Fung et al. 1992). However, whereas SIR-C/X-SAR was providing multi-frequency SAR imagery acquired simultaneously, current spaceborne SAR sensors operate at single frequencies, and as a consequence, SAR data from different satellites have to be used for multi-frequency SAR classification purposes. Because they are usually acquired with a considerable time lag in between, a profound knowledge of the radar backscatter properties of the sediment types, and their dependence on weather conditions, tidal cycle, and imaging geometry is needed, which can only be gained from a joint analysis of multi-satellite SAR data and optical remote sensing data, together with a-priori knowledge gained during in-situ campaigns.

The data acquired at different radar bands (L, C, and X band, from ALOS PALSAR, ERS SAR, Radarsat-2 and ENVISAT ASAR, and TerraSAR-X, respectively) have been used to analyse their potential for crude sediment classification on dry-fallen intertidal flats and for detecting benthic fauna such as blue mussel or oyster beds

## 2. AREAS OF INTEREST

Three main test areas on the German North Sea coast were identified (Fig. 1), which represent areas of typical sediment distribution on intertidal flats, but also include vegetated areas and mussel and oyster beds. During summer season, some regions are covered by sea grass and green algae. Thus, a simple classification method that assumes bare sediments cannot be applied in those areas.

The test area “Norderney” is part of the German National Park “Lower Saxony Wadden Sea”, in the south-western part of the German North Sea coast (area “A” in Fig. 1). It covers the intertidal range on the backside of the island of Norderney, between the island

and the mainland. From the eastern center of the test site two tidal channels emerge, with several smaller tidal creeks entering into them from the south (lower panel of Fig. 4). The test site is dominated by a strong spatial variation of different sediment types: the upper soil layer mainly consists of sandy sediments, but also muddy areas can be found in the eastern center, at the watershed between the two tidal channels. Large areas in the site's center are covered by blue mussels [*mytilus edulis*] and Pacific oysters [*crassostrea gigas*], the latter having invaded into that part of the Wadden Sea only recently.

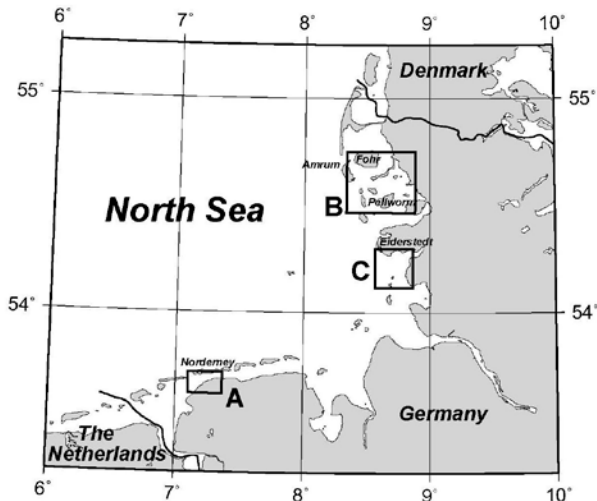


Figure 1. The three test sites of this study. “Norderney” (A) is located between the island of Norderney and the mainland, “Halligenwatt” (B) lies between the Northern Frisian islands Amrum, Föhr, and Pellworm, and “Wesselburener Watt” (C) is located south of the Eiderstedt peninsula.

Fig. 2 demonstrates how the test site is imaged by SAR sensors working at different radar bands: the upper panel shows an ALOS PALSAR (L-band) image acquired on April 12, 2008, at 21:43 UTC, 23 minutes after low tide, and the lower panel shows a TerraSAR-X (X-band) image acquired on August 30, 2008, at 17:10 UTC, 34 minutes after low tide. The location of the tidal creeks can be identified through enhanced radar backscattering from the sediment on their edges. Some irregular bright patches in the left part of both SAR images are not due to sand ripples, but due to mussel beds. The mussels, sticking out of the sediments, increase the surface roughness locally, and this is why they are visible on SAR imagery. It is worth noting that, for the first time, benthic fauna on exposed intertidal flats has been identified on multi-frequency (L, C, and X band) SAR images of that area.

The test site “Halligenwatt” (area “B” in Fig. 1) lies in the German National Park “Schleswig-Holstein Wadden Sea”, in the northern part of the German North Sea coast. It is bordered by the islands of Amrum and Föhr

in the west and north, respectively, and by the mainland in the east. This test area also includes the island of Pellworm in the south (Fig. 1) and several small, undiked islands, called “Hallig”, which are frequently flooded during strong high tide or storm surges. Similar to the southern test site in Lower Saxony, the spatial variations of different sediment types, along with the occurrence of mussel beds, sea grass, and macro algae, are typical for the test site “Halligenwatt” in Schleswig-Holstein. Sandy sediments dominate the entire test area and during the vegetation period in late spring and summer, large areas are covered by sea grass. Muddy sediments are mainly found along the coast.

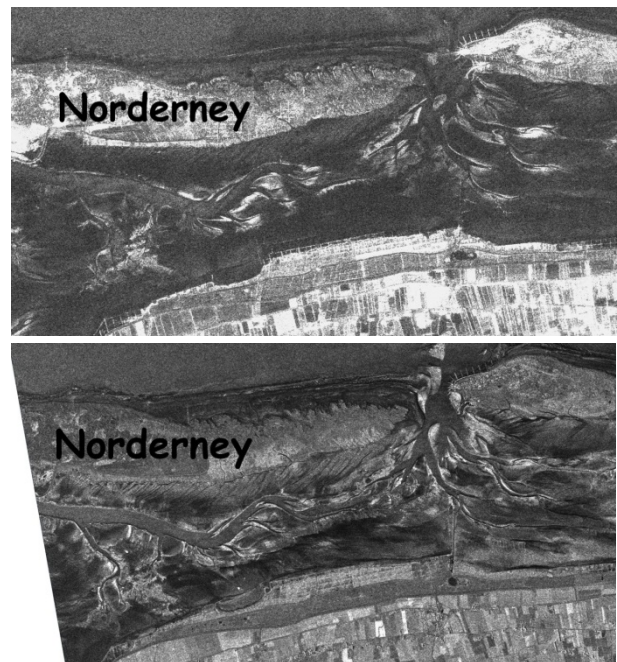


Figure 2. Two SAR images (25.7 km × 13.4 km) of the test site “Norderney”, acquired shortly after low tide. Top: ALOS PALSAR image of 12 April 2008, 21:43 UTC (© JAXA 2008); bottom: TerraSAR-X image of 30 August 2008, 17:10 UTC (© DLR 2008).

The third test area, “Wesselburen” (area “C” in Fig. 1), covers the intertidal range south of the Eiderstedt peninsula on the Schleswig Holsteinean North Sea coast. This area has been subject of frequent field excursions and was already imaged by SIR-C/X-SAR in 1994 (Gade et al. 2008). Except for elongated areas on the coast, which are covered by seagrass during the vegetation period, this test area can be considered unvegetated. The sediments are mainly sandy, while muddy areas are only found at the (narrow) arms of the tidal creeks and along the coast. Two SAR images of that test site are shown in Fig. 3. The upper one was acquired by TerraSAR-X on 30 September 2009 at 17:10 UTC, 130 minutes after low tide. The lower one was acquired by Radarsat-2 on 17 October 2009, at 16:56 UTC, 14 minutes before low tide. In both SAR

images bright areas (due to increased NRCS) appear at the same locations, mainly along the branches of the tidal creeks and on the outer (sandy) tidal flats. Thus, even though the SAR images were acquired at different polarizations (TerraSAR-X at VV, Radarsat-2 at HH), we note that the imaging of exposed intertidal flats is similar at C and X band, which is in accordance with the observations by Gade et al. (2008).

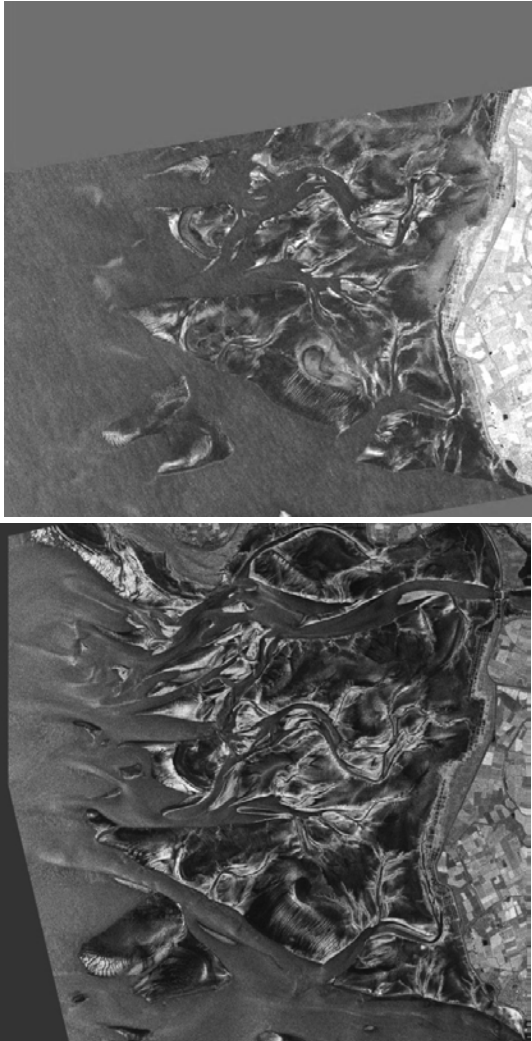


Figure 3. Two SAR images of the test site “Wesselburen”, acquired close to low tide. Top: TerraSAR-X image of September 30, 2009, 17:10 UTC (© DLR 2009); bottom: Radarsat-2 image of October 17, 2009, 16:56 UTC (© CSA 2009).

### 3. EXISTING CLASSIFICATION SYSTEM

Optical sensors are already being used for sediment and habitat classification on intertidal flats and promising results have been achieved through the classification of different sediment types, vegetation, and mussel beds (Brockmann and Stelzer 2008). Existing classification systems for the different surface types of intertidal flats are usually based upon optical remote sensing data,

since the multi-channel (hyperspectral) data allow for a classification of a large number of surface types (classes). The method applied is built upon linear spectral unmixing and feature extraction from the spectral reflectances (Brockmann and Stelzer 2008). All extracted information from the optical data is combined in a decision tree, which is used to relate each pixel to a class representing nine surface types, i.e., five sediment types, two vegetation density classes, one mussel class, and a class representing dry and bright sands. The water coverage, having a strong influence on both the spectral reflectance and the radar backscattering, is considered within the end-member selection for the linear spectral unmixing. Fig. 4 shows examples for the three test sites on the German North Sea coast (Fig. 1).

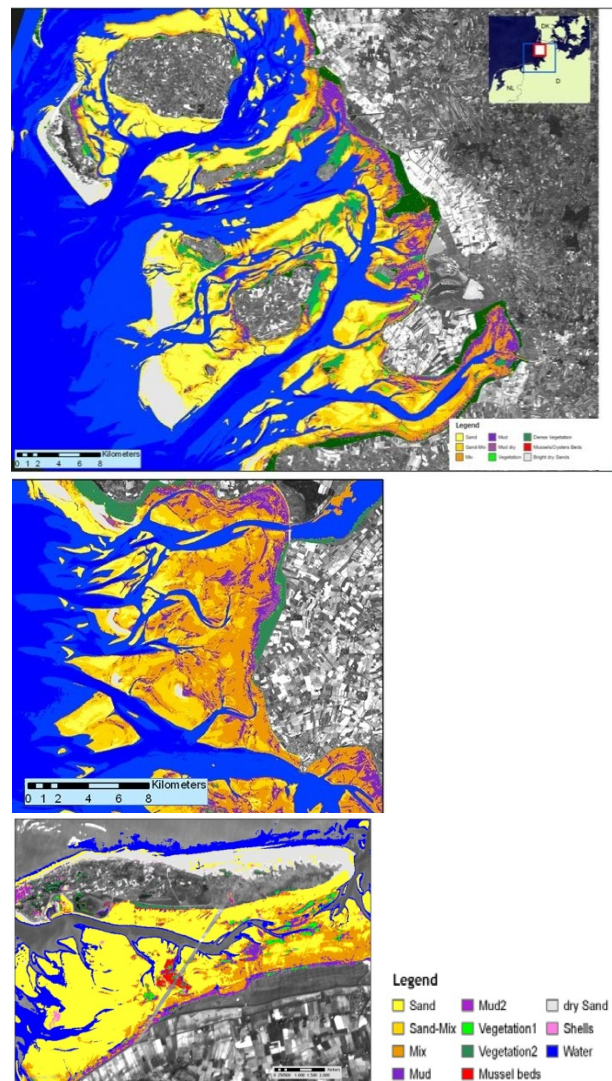


Figure 4. Sediment classification for the three test sites of interest, “Halligenwatt”, “Wesselburen” and “Norderney” (top to bottom) based on SPOT-4 data acquired in July 2006 and August 2008 (original data © SPOT Image 2006, 2008, data processing © Brockmann Consult 2008).

#### 4. SAR DATA ANALYSES

A total of 120 SAR images acquired over the three test sites of this study were analysed with respect to the information content, which can be gained from radar imagery of exposed intertidal flats, and which can enter into existing classification and monitoring schemes. Table 1 provides an overview of the SAR images used for the present investigation.

Table 1. SAR scenes used for the present investigation.

Satellite / Sensor	Pixel Size	Polarization	Images
ENVISAT ASAR	12.5 m	VV	23
ERS-2 SAR	12.5 m	VV	23
ALOS PALSAR	6.25 m	HH, HV	4
	12.5 m		15
Radarsat-2	100 m	HH	2
	1.6 m		1
TerraSAR-X	0.5 m	VV, HH	20
	0.75 m		9
	1.0 m		17
	1.25 m		6

##### 4.1. Multi-satellite SAR data

In order to derive surface roughness parameters we have performed an inversion of the Integral Equation Model (Fung et al. 1992, Fung and Chen 2004) in the same way as proposed by Gade et al. (2008). For a given imaging geometry (i.e., incidence angle and look direction), and assuming the sediments on exposed intertidal flats to be mostly saturated with water, the most likely roughness parameters can be inferred using the NRCS values at two different radar bands and applying an inversion of the IEM (Gade et al. 2008, Deroin 2012). We note, however, that the different acquisition times and imaging geometries may result in additional constraints.

In Fig. 5 maps of the correlation length (upper panel) and the rms height (lower panel) for the northern-most test site “Halligenwatt” are shown, as derived through the IEM inversion using an ALOS PALSAR scene and the ENVISAT ASAR scene of 18 October 2007. The images were acquired at 09:55 UTC (ASAR), 87 minutes before low tide, and at 21:36 UTC (PALSAR), 110 minutes before low tide, respectively. The applied land-and-water mask was derived using cross-polarization PALSAR imagery, which is well suited for waterline detection (Deroin 2012). While the derived rms heights vary only slightly over the entire test site, with local maxima only at the edges of the tidal creeks, the correlation lengths are largest in those areas, which have been classified as sandy (upper panel in Fig. 4). This is in agreement with earlier findings by Gade et al.

(2008), who performed a crude sediment classification based on maps of the surface correlation length.

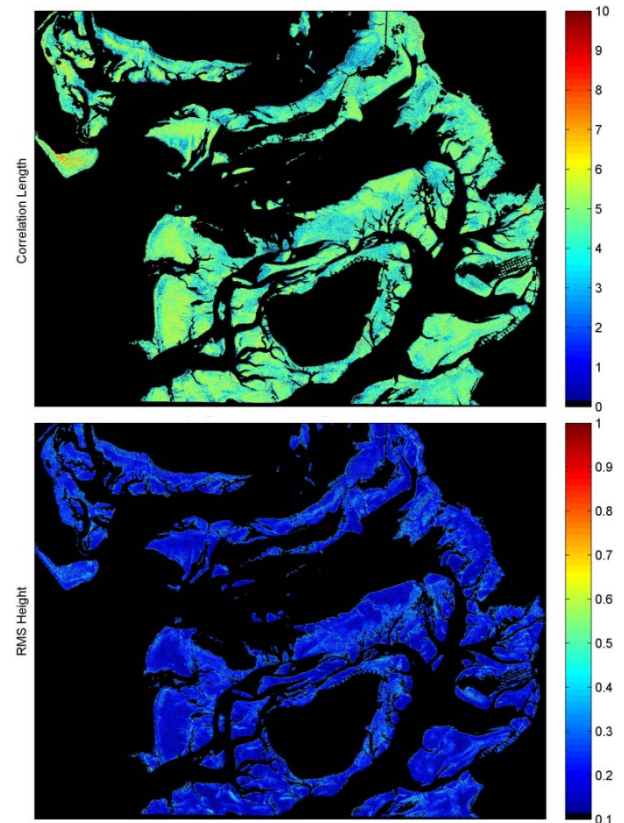


Figure 5. Results of the IEM inversion for the northern test area “Halligenwatt”, based on an ALOS PALSAR image of 18 October 2007 (21:36 UTC, 110 minutes before low tide) and an ENVISAT ASAR image of the same day (09:55 UTC, 87 minutes before low tide).

Top: correlation lengths, bottom: rms heights.

We performed a statistical analysis of the IEM inversion results for all test areas, in order to find out to what extent the derived results are stable and/or their variation can be used to gain further information on the surface properties. Fig. 6 shows simple statistical parameters, the mean values (left column) and standard deviations (right column), for the correlation length (upper row) and rms height (lower row), as derived from 140 inversions performed for the test area “Wesselburen”.

We found no strong variation of the mean correlation lengths (upper left panel), which can be explained by the generally sandy sediments (middle panel of Fig. 4). Larger values of the mean rms height (lower left panel of Fig. 6) can be found close to the tidal creeks, which can be explained by a variation of the water level (and thus in the water line), by remnant water on the exposed flats, and by a higher sensitivity to the SAR look direction relative to the local orientation of the creek edges. The mean rms heights are smallest in sandy

areas. Finally, the standard deviations of both the correlation lengths and the rms heights show a similar spatial variation (right column of Fig. 6), with maximum values in the vicinity of the tidal creeks.

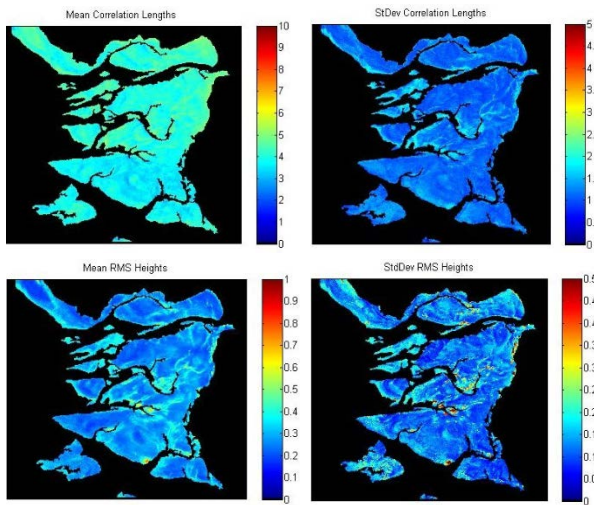


Figure 6. Statistical analysis of 140 IEM inversions performed for the test area “Wesselburen”. Upper row: correlation length, lower row: rms height; left column: mean values, right column: standard deviations.

#### 4.2. Multi-temporal SAR data

The wealth of SAR images available for the present study allows not only for the derivation of surface roughness parameters through the IEM inversion, and using multi-satellite SAR data. Moreover, we used single-satellite SAR data to infer information on the kind of scatterers responsible for the observed SAR image signatures.

The extended mussel beds in the test area “Norderney” cause bright signatures in nearly every SAR image acquired over that area, independent of the imaging geometry (incidence angle and radar look direction). Therefore, multi-temporal analyses of single-satellite SAR images may also yield valuable information on the occurrence and the extent of mussel beds that can enter into existing monitoring systems. Fig. 7 demonstrates an example.

We have used four TerraSAR-X images of 2009 (acquired between 1 h before, and 1 h after low tide) and have calculated the mean values and standard deviations of the normalized radar cross section (NRCS) on a pixel-by-pixel basis. Green areas in Fig. 7 correspond to a large mean NRCS and a small standard deviation; in white areas both the mean NRCS and its standard deviation are large. Because of their isotropic roughness the mussel beds, apart from the land and some other areas, can be easily separated from the other bright areas in their vicinity, which may, or may not, cause an enhanced NRCS, depending on imaging geometry and environmental conditions. Thus, it is

obvious that such (simple) statistical analyses can help identifying mussel (and oyster) beds, because of the generally higher surface roughness in those areas.

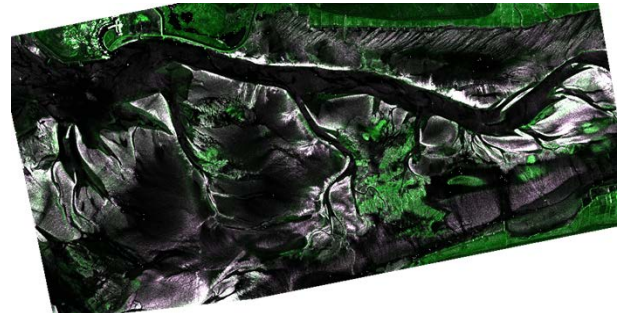


Figure 7. Indicators for mussel beds in the test site “Norderney”, derived through a statistical analysis of four TerraSAR-X images of 2009 (acquired between 1 h before low tide and 1 h after low tide). Green colour marks high mean NRCS and low NRCS standard deviation. White colour marks high mean NRCS and high NRCS standard deviation. Oyster and (blue) mussel beds can be delineated in the image center.

#### 4.3. Archaeological observations

In the Middle Ages, farmsteads and villages existed along the Northern Frisian North Sea coast, surrounded by farmland and floodplain forests (Bantelmann et al. 1995). The houses were mostly built on dwelling mounds, protected by small dikes, and ditches were built to take out the water of the farmlands. Large areas were lost to the sea during major storm surges in the 14th and 17th century, the second of which, the so-called big (second) “Manndränke” is still the most known storm surge in history in the area of the North Frisian Wadden Sea. Major parts of the populated coastal area were destroyed and the swampy land changed its face and became the Wadden Sea as it is known today (Behre 2009). Foundations of farm houses or stables, but also remnants of ditches or lanes were buried by fine sediments, but may show up again, when the topmost sediment layer is driven apart under the action of currents and waves. These sedimental structures show distinct biological effects and are often marked by benthic organisms.

We analyzed the high-resolution TerraSAR-X imagery of the “Halligenwatt” test area with respect to the imaging of residuals of former land use. As an example, the upper panel of Fig. 8 shows a part of a TerraSAR-X scene acquired on 3 August 2009 over the intertidal flats north of the island of Pellworm (in the center of the Halligenwatt test area). Diagonal bright and dark lines can be delineated in the lower left and upper right image center, respectively, which are different from the latticed signatures along the coast, which in turn are due to land reclamation. For comparison, an existing map of farmland residuals in that area, as provided by the Schleswig Holstein State Archaeological Office, is

shown in the lower panel of Fig. 8. It is obvious that the observed diagonal lines in the SAR image coincide with residuals of former farmland ditches, which are marked as blue lines.

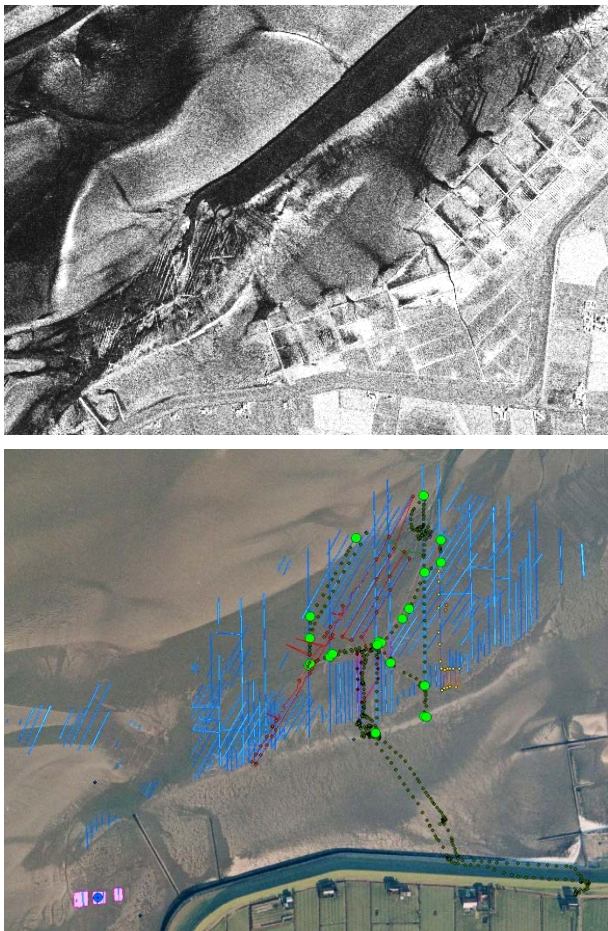


Figure 8. Top: subsection (2.8 km  $\times$  2.0 km) of a TerraSAR-X image of intertidal flats north of the island of Pellworm in the “Halligenwatt” test area, acquired on 3 August 2009 (05:42 UTC, 54 minutes after low tide). © DLR 2009. Bottom: Aerial photograph of the same area, with the locations of residuals of historical land use superimposed.

High-resolution TerraSAR-X images can be used to complement archaeological surveys in those areas, since the radar is capable of imaging the former systems of ditches dating back to the 17th century. The observed signatures are due to different sediment types, which in turn are due to the very ditch morphology. Thus, historical ditch structures, which are still containing more biogenic material than the surrounding sediments, may be a preferred habitat of certain mussels while sand worms (*Arenicola marina*) are usually found on sandy sediments. Those benthic organisms may cause different surface roughness patterns that can be sensed by the high-resolution X-Band SAR. For more details on our

ongoing investigations the reader is referred to Gade and Kohlus (2011).

## 5. SUMMARY AND CONCLUSIONS

Data from optical sensors and multi-satellite SAR images of exposed intertidal flats have been analyzed to improve existing classification systems by including SAR data. We have demonstrated that a systematic analysis of SAR data from exposed intertidal flats, acquired close to low tide, provides additional information to be used for the routine monitoring of the German Wadden Sea. For the first time, SAR images from multiple satellites were used to derive maps of surface roughness parameters, namely the (auto-) correlation length and the rms height of the sediment surface.

Our results presented herein show evidence that even SAR data, which were acquired with a considerable time lag in between, can be used for an inversion of the Integral Equation Model (IEM), which provided reasonable qualitative and quantitative results.

In general, SAR data to be used for the monitoring of dry-fallen intertidal flats should be acquired between one hour before and two hours after low tide. However, since remnant water on the exposed flats may affect the classification (using both optical and microwave sensors), SAR data acquired well after low tide are best suited for the analyses reported herein. We also note that the water level at the very place under investigation strongly depends on environmental (weather) conditions. Thus, a profound knowledge of all main factors contributing to the observed SAR signatures is essential for any improvement of existing classification systems.

For the first time, extensive mussel beds (composed of a mixture of Pacific oysters and blue mussels) have been observed in multi-frequency SAR imagery. However, the strength of their signatures, and thus the capability of SAR sensors to detect and to classify them, may depend on the seasonal change in coverage by brown algae.

The integration of SAR data into an existing classification system results in a significant improvement of the classification of different surface types, particularly of mussel or oyster beds, which can be detected at all deployed frequency bands, i.e. by all sensors used. In this frame, our statistical, multi-temporal analyses provided most promising results. The joint processing of SAR images of various sensors, working at different radar frequencies, has shown that surface roughness parameters can be obtained through the inversion of the Integral Equation Model (IEM), even when the input data were acquired at different times and from different platforms. The information gained from the optical and SAR sensors, along with in-situ observations, is used to improve an existing classification system.

In addition to the routine sediment classification, for the first time, data from the high-resolution TerraSAR-X are used to demonstrate that residuals of former settlements and agricultural areas, lost during storm surges in the 14th and 17th centuries, can be detected from space. This finding has provided a completely new application field for SAR data, since such residuals haven't been observed on satellite imagery so far, and the analysis of TerraSAR-X data has already enhanced the knowledge about land use residuals, which were so far unknown. The SAR data are complemented by aerial photographs and in-situ data.

The applicability of our algorithm, to use multi-satellite SAR data acquired at L band and at either C band or X band, depends on the availability of the respective SAR data. After ALOS, ERS-2 and ENVISAT have are no longer in operation, only C and X band SAR data will be routinely available in the near future, e.g. from Radarsat-2, Sentinel-1, TerraSAR-X, and Cosmo-Skymed. A lack of L-band SAR data, however, will strongly limit the possibilities demonstrated herein, and future studies will have to focus on the use of (polarimetric) SAR data acquired at C and X band.

#### ACKNOWLEDGMENTS

The authors are grateful to the colleagues of the German national project DeMarine-Umwelt (Environment), sub-project 4, who contributed to the results presented herein. DMU receives funding from the German Ministry of Economy (BMWi) under contract 50 EE 0817, TSX data were provided by DLR under contract COA0118.

#### REFERENCES

- Bantelmann, A., R. Kuschert, A. Panten, and T. Steensen (1995): "Geschichte Nordfrieslands", Boyens, Heid, 472 pp.
- Behre, K.-H. (2009): "Landschaftsgeschichte Norddeutschlands: Umwelt und Siedlung von der Steinzeit bis zur Gegenwart", Wachholtz, Neumünster, 308 pp.
- Brockmann, C., and K. Stelzer (2008). "Optical Remote Sensing of Intertidal Flats", in "Remote Sensing of the European Seas", V. Barale and M. Gade (Eds.), Springer, Heidelberg, pp. 117-128.
- Deroin, J.-P. (2012), Combining ALOS and ERS-2 SAR data for the characterization of intertidal flats. Case study from the Baie des Veys, Normandy, France. *Int. J. Earth Observ. Geoinf.*, 18, 183-194.
- Fung, A.K. and K.S. Chen (2004), An update on the IEM surface backscattering model. *IEEE Geosci. Remote Sens. Letters*, 1, 75-77.
- Fung, A. K., Z. Li, and K.S. Chen (1992), "Backscattering from a Randomly Rough Dielectric Surface", *IEEE Trans. Geosci. Remote Sens.*, 30, 356-369.
- Gade, M., W. Alpers, C. Melsheimer, and G. Tanck (2008). "Classification of sediments on exposed tidal flats in the German Bight using multi-frequency radar data", *Remote Sens. Environ.*, vol. 112, pp. 1603-1613.
- Gade, M., and J. Kohlus (2011), "Archeological Sites on Intertidal Flats in the German Wadden Sea", *Proceed. 4th TSX Science Team Meeting, Oberpfaffenhofen, Germany, 14-16 February 2011, DLR Publications.*